Video Article

The Bioconjugation and Radiosynthesis of ^{89}Zr-DFO-labeled Antibodies

Brian M. Zeglis[1], Jason S. Lewis[1]

[1]Department of Radiology, Memorial Sloan Kettering Cancer Center

Correspondence to: Jason S. Lewis at lewisj2@mskcc.org

URL: http://www.jove.com/video/52521
DOI: doi:10.3791/52521

Keywords: Chemistry, Issue 96, Positron Emission Tomography, Antibody, Bioconjugation, Immunoconjugates, Desferrioxamine, ^{89}Zr

Date Published: 2/12/2015

Citation: Zeglis, B.M., Lewis, J.S. The Bioconjugation and Radiosynthesis of ^{89}Zr-DFO-labeled Antibodies. *J. Vis. Exp.* (96), e52521, doi:10.3791/52521 (2015).

Abstract

The exceptional affinity, specificity, and selectivity of antibodies make them extraordinarily attractive vectors for tumor-targeted PET radiopharmaceuticals. Due to their multi-day biological half-life, antibodies must be labeled with positron-emitting radionuclides with relatively long physical decay half-lives. Traditionally, the positron-emitting isotopes ^{124}I ($t_{1/2}$ = 4.18 d), ^{86}Y ($t_{1/2}$ = 14.7 hr), and ^{64}Cu ($t_{1/2}$ = 12.7 hr) have been used to label antibodies for PET imaging. More recently, however, the field has witnessed a dramatic increase in the use of the positron-emitting radiometal ^{89}Zr in antibody-based PET imaging agents. ^{89}Zr is a nearly ideal radioisotope for PET imaging with immunoconjugates, as it possesses a physical half-life ($t_{1/2}$ = 78.4 hr) that is compatible with the *in vivo* pharmacokinetics of antibodies and emits a relatively low energy positron that produces high resolution images. Furthermore, antibodies can be straightforwardly labeled with ^{89}Zr using the siderophore-derived chelator desferrioxamine (DFO). In this protocol, the prostate-specific membrane antigen targeting antibody J591 will be used as a model system to illustrate (1) the bioconjugation of the bifunctional chelator DFO-isothiocyanate to an antibody, (2) the radiosynthesis and purification of a ^{89}Zr-DFO-mAb radioimmunoconjugate, and (3) *in vivo* PET imaging with an ^{89}Zr-DFO-mAb radioimmunoconjugate in a murine model of cancer.

Video Link

The video component of this article can be found at http://www.jove.com/video/52521/

Introduction

Due to their remarkable sensitivity, affinity, and selectivity, antibodies have long been considered promising vectors for the delivery of radioisotopes to cancer cells. However, their application in positron emission tomography (PET) imaging has been hampered by the lack of a suitable positron-emitting radioisotope for their labeling.[1-3] One of the most critical considerations in the design of radioimmunoconjugates is matching the physical decay half-life of the radioisotope to the *in vivo* pharmacokinetics of the antibody. More specifically, antibodies often have relatively long, multi-day biological half-lives and therefore must be labeled with radioisotopes with comparable physical half-lives. For PET imaging applications, antibodies have traditionally been radiolabeled with ^{64}Cu ($t_{1/2}$ = 12.7 hr), ^{86}Y ($t_{1/2}$ = 14.7 hr), or ^{124}I ($t_{1/2}$ = 4.18 d).[4,5] However, each of these radioisotopes possesses significant limitations that hamper their suitability for clinical imaging. While radioimmunoconjugates labeled with ^{86}Y and ^{64}Cu have proven promising in preclinical investigations, both isotopes possess physical half-lives that are too short to be effective for imaging in humans. ^{124}I, in contrast, has a nearly ideal physical half-life for imaging with antibodies, but it is expensive and has suboptimal decay characteristics that lead to relatively low resolution clinical images. Furthermore, ^{124}I-labeled radioimmunoconjugates can be subject to dehalogenation *in vivo*, a process which can lower tumor-to-background activity ratios.[6,7]

The drive to find a positron-emitting radioisotope to supplant ^{64}Cu, ^{86}Y, and ^{124}I in radioimmunoconjugates has fueled the recent surge in research on ^{89}Zr-labeled antibodies.[8-12] The reason for the advent of ^{89}Zr is straightforward: the radiometal possesses near-ideal chemical and physical properties for use in diagnostic PET radioimmunoconjugates.[13] ^{89}Zr is produced via the ^{89}Y(p,n)^{89}Zr reaction on a cyclotron using a commercially available and 100% naturally abundant ^{89}Y target.[14,15] The radiometal has a positron yield of 23%, decays with a half-life of 78.4 hr, and emits positrons with the relatively low energy of 395.5 keV (**Figure 1**).[13,16,17] It is important to note that ^{89}Zr also emits a high energy, 909 keV γ-ray with 99% efficiency. While this emission *does not* interfere energetically with the emitted 511 keV photons, it does require extra consideration with regard to transport, handling, and dosimetry. Despite this caveat, these decay characteristics ultimately mean that ^{89}Zr not only has a more favorable half-life for imaging with antibodies than ^{86}Y and ^{64}Cu but can also produce higher resolution images than ^{124}I, which emits positrons with higher energies of 687 and 975 keV as well as a number of photons with energies within 100-150 keV of the 511 keV positron-created photons.[13] Moreover, ^{89}Zr is also safer to handle, less expensive to produce, and residualizes in tumors more effectively than its radioiodine counterpart.[18,19] One potential limitation of ^{89}Zr is that it does not have a therapeutic isotopologue, *e.g.*, ^{86}Y (PET) vs. ^{90}Y (therapy). This precludes the construction of chemically identical, surrogate imaging agents that can be employed as dosimetric scouts for their therapeutic counterparts. That said, investigations suggest that ^{89}Zr-labeled antibodies do have potential as imaging surrogates for ^{90}Y- and ^{177}Lu-labeled immunoconjugates.[20,21]

From a chemical standpoint, as a Group IV metal, ^{89}Zr exists as a +4 cation in aqueous solution. The Zr^{4+} ion is highly charged, relatively large (effective ionic radius = 0.84 Å), and can be classified as a “hard” cation. As such, it exhibits a preference for ligands bearing up to eight hard, anionic oxygen donors. Easily the most common chelator used in ^{89}Zr-labeled radioimmunoconjugates is desferrioxamine (DFO), a

siderophore-derived, acyclic chelator bearing three hydroxamate groups. The ligand stably coordinates the Zr^{4+} cation quickly and cleanly at RT at biologically relevant pH levels, and the resulting Zr-DFO complex remains stable over the course of multiple days in saline, blood serum, and whole blood.[22] Computational studies strongly suggest that DFO forms a hexacoordinate complex with Zr^{4+} in which the metal center is coordinated to the three neutral and three anionic oxygen donors of the ligand as well as two exogenous water ligands (**Figure 2**).[23,24] The *in vivo* behavior of radioimmunoconjugates employing the ^{89}Zr-DFO conjugation scaffold has generally been excellent. However, in some cases, imaging and acute biodistribution studies have revealed elevated activity levels in the bones of mice injected with ^{89}Zr-labeled antibodies, data that suggests that the osteophilic $^{89}Zr^{4+}$ cation is released from the chelator *in vivo* and subsequently mineralizes in the bone.[25] Recently, a number of investigations into the development of novel $^{89}Zr^{4+}$ chelators particularly ligands with eight oxygen donors have appeared in the literature.[24,26,27] Nevertheless, at present, DFO is the most widely employed chelator in ^{89}Zr-labeled radioimmunoconjugates by a wide margin. A variety of different bioconjugation strategies have been employed to attach DFO to antibodies, including bioorthogonal click chemistry, the reaction of thiol-reactive DFO constructs with cysteines in the antibody, and the reaction of activated ester-bearing DFO constructs with lysines in the antibody.[4,28-30] Easily the most common strategy, however, has been the use of an isothiocyanate-bearing derivative of DFO, DFO-NCS (**Figure 2**).[22] This commercially available bifunctional chelator robustly and reliably forms stable, covalent thiourea linkages with the lysines of the antibody (**Figure 3**).

Over the past few years, a wide variety of ^{89}Zr-DFO-labeled radioimmunoconjugates have been reported in the literature. Preclinical investigations have been especially abundant, featuring antibodies ranging from the more well-known cetuximab, bevacizumab, and trastuzumab to more esoteric antibodies such as the CD105-targeting TRC105 and fPSA-targeting 5A10.[30-36] More recently, a small number of early-phase clinical trials using ^{89}Zr-DFO-labeled antibodies have emerged in the literature. Specifically, groups in the Netherlands have published trials employing ^{89}Zr-DFO-cmAb U36, ^{89}Zr-DFO-ibritumomab tiuxetan, and ^{89}Zr-DFO-trastuzumab.[21,32,37] In addition, a range of other clinical trials with ^{89}Zr-labeled radioimmunoconjugates are currently underway, including investigations here at Memorial Sloan Kettering Cancer Center using the PSMA-targeting ^{89}Zr-DFO-J591 for prostate cancer imaging and the HER2-targeting ^{89}Zr-DFO-trastuzumab for breast cancer imaging.[23,30] In addition, while radiolabeled antibodies remain the most common ^{89}Zr-labeled radiopharmaceuticals, the radiometal has also increasingly been employed with other vectors, including peptides, proteins, and nanomaterials.[38-43]

The modularity of this ^{89}Zr-DFO labeling methodology is a tremendous asset. The repertoire of biomarker-targeting antibodies is ever-expanding, and the interest in performing *in vivo* PET imaging using these constructs is growing apace. As a result, we believe that the development of more standardized practices and protocols could benefit the field. An excellent written experimental protocol for DFO-NCS conjugation and ^{89}Zr radiolabeling has already been published by Vosjan, *et al.*[22] We feel that the visual demonstration provided by this work could further help investigators new to these techniques. In the protocol at hand, the prostate-specific membrane antigen targeting antibody J591 will be used as a model system to illustrate (1) the bioconjugation of the bifunctional chelator DFO-isothiocyanate to an antibody, (2) the radiosynthesis and purification of the ^{89}Zr-DFO-mAb radioimmunoconjugate, and (3) *in vivo* PET imaging with a ^{89}Zr-DFO-mAb radioimmunoconjugate in a murine model of cancer.[23,44,45]

Protocol

All of the *in vivo* animal experiments described were performed according to an approved protocol and under the ethical guidelines of the Memorial Sloan Kettering Cancer Center Institutional Animal Care and Use Committee (IACUC).

1. Conjugation of DFO-NCS to J591

1. In a 1.7 ml microcentrifuge tube, prepare a 2-5 mg/ml solution of J591 in 1 ml of either 1x phosphate-buffered saline (pH 7.4) or 0.5 M HEPES buffer (pH 7.4).
2. Dissolve DFO-NCS in dry DMSO at a concentration between 5-10 mM (3.8-7.6 mg/ml). Sonicate or vortex the solution thoroughly in order to facilitate complete dissolution.
3. Adjust the pH of the J591 solution to 8.8-9.0 by adding small aliquots (< 10 µl) of 0.1 M Na_2CO_3.
4. Once the antibody solution is at the correct pH, add a volume of the DFO-NCS solution corresponding to a 3-4-fold molar excess of the bifunctional chelator.
    1. For example, add 4-5 µl of a 10 mM (7.6 mg/ml) DFO-NCS solution (40.4 nmol DFO-NCS) to 1 ml of a 2 mg/ml J591 antibody solution (13.3 nmol J591). The amount of DMSO in the final aqueous reaction mixture should not exceed 2% v/v.
5. Incubate the reaction for 30 min at 37 °C on an agitating heating block at 350 rpm.
6. After 1 hr at 37 °C, purify the resulting immunoconjugate using a pre-packed disposable size exclusion desalting column with a 50,000 molecular weight cut-off using 0.5 M HEPES buffer (pH 7.4) as the eluent. This step will yield a 2 ml solution of the completed J591-DFO construct.
7. Measure the concentration of the J591-DFO construct on a UV-Vis spectrophotometer.
8. If a higher concentration of the construct is desired, concentrate the J591-DFO solution using a centrifugal filter unit with a 50,000 molecular weight cut-off.
9. Store the solution of the completed J591-DFO immunoconjugate at -20 °C in the dark.
   NOTE: This is an acceptable stopping point in the procedure.

2. Radiolabeling J591-DFO with ^{89}Zr

CAUTION: This step of the protocol involves the handling and manipulation of radioactivity. Before performing these steps or performing any other work with radioactivity researchers should consult with their home institution's Radiation Safety Department. All possible steps should be taken to minimize exposure to ionizing radiation.

NOTE: In the interest of proper radiochemical note-keeping, the amount of radioactivity in the sample should be measured using a dose calibrator and recorded before and after Steps 2.2-2.13 in the protocol below. This will help with the accurate determination of radiochemical yields and specific activities.

1. Prepare a solution of 0.5-2.0 mg of J591-DFO in 200 µl of 0.5 M HEPES buffer, pH 7.5.
2. Pipette a volume of the $^{89}Zr^{4+}$ stock solution (typically supplied in 1.0 M oxalic acid) corresponding to 1.0-6.0 mCi (37-222 MBq) into a 2 ml plastic screw-cap microcentrifuge tube. Adjust the volume of this solution to a total 300 µl using 1.0 M oxalic acid.
3. Adjust the pH of the $^{89}Zr^{4+}$ solution to 6.8-7.5 using 1.0 M Na_2CO_3. Begin by adding 250 µl of 1.0 M Na_2CO_3 to the $^{89}Zr^{4+}$ solution and subsequently add smaller (< 10 µl) aliquots of base to achieve the desired pH.
4. Add the desired amount of pH-adjusted $^{89}Zr^{4+}$ solution to the J591-DFO solution prepared in Step 2.1.
5. Check the pH of the radiolabeling reaction mixture to ensure that it falls within the desired range of 6.8-7.5.
6. Incubate the radiolabeling reaction for 60 min at RT on an agitating heating block at 350 rpm.
7. After 60 min of incubation, measure the radiolabeling yield of the reaction using radio-TLC.
    1. To this end, spot 1 µCi of the radiolabeling reaction mixture on a silica-impregnated TLC strip. Allow the aliquot to dry, run the TLC using an eluent of 50 mM DTPA (pH 5.5) and analyze the TLC strip using a radio-TLC scanner. $^{89}Zr^{4+}$ bound to the J591-DFO construct will appear at the origin (R_f < 0.1), while free $^{89}Zr^{4+}$ cations will be chelated by DTPA and will elute with the solvent front (R_f > 0.9).
    2. Calculate the radiolabeling yield of the reaction by integrating the radiochromatogram, dividing the area under the curve from R_f 0.0-0.1 by the total area under the curve, and multiplying by 100.
8. If the radiolabeling yield is sufficient (typically a theoretical specific activity of >2 mCi/mg), quench the reaction with 5 µl of 50 mM DTPA, pH 5.5.
9. Purify the resulting immunoconjugate using a pre-packed disposable size exclusion desalting column with a 50,000 molecular weight cut-off using an eluent of either 0.9% sterile saline with 5 mg/ml gentisic acid or 0.25 M sodium acetate (pH 5.5) with 5 mg/ml gentisic acid. This step will yield a 2 ml solution of the completed ^{89}Zr-DFO-J591 radioimmunoconjugate.
10. After purification, verify the radiochemical purity of the ^{89}Zr-DFO-J591 using radio-TLC as described in Step 2.7.
11. Calculate the overall radiolabeling yield of the reaction by dividing the amount of activity initially added to the antibody solution by the amount of radioactivity isolated with the purified ^{89}Zr-DFO-J591 radioimmunoconjugate.
12. Calculate the final specific activity by dividing the amount of activity isolated with the purified ^{89}Zr-DFO-J591 radioimmunoconjugate by the initial mass of DFO-J591 in the radiolabeling reaction.
13. If a higher concentration is desired, concentrate the ^{89}Zr-DFO-J591 solution using a centrifugal filter unit with a 50,000 molecular weight cut-off.
    NOTE: The gentisic acid used in the final purification step is a radio-protectant employed to minimize the degradation of the antibody due to radiolysis.[46] While the storage of the ^{89}Zr-DFO-J591 radioimmunoconjugate for up to 48 hr at 4 °C is possible, it is not recommended. If the radioimmunoconjugate is to be stored, use 0.25 M sodium acetate (pH 5.5) with 5 mg/ml gentisic acid as the storage buffer in order to minimize the risk of hypochlorite-mediated radiolysis.[47]

3. *In Vivo* PET Imaging with ^{89}Zr-DFO-J591

CAUTION: As in Protocol Section 2, this step of the protocol involves the handling and manipulation of radioactivity. Before performing these steps researchers should consult with their home institution's Radiation Safety Department. All possible steps should be taken to minimize exposure to ionizing radiation.

1. In male athymic nude mice, subcutaneously implant 5 x 10^6 LNCaP prostate cancer cells and allow these to grow to a 100-150 mm^3 xenograft (3-4 weeks after inoculation).[44]
2. Dilute the ^{89}Zr-DFO-J591 radioimmunoconjugate to a concentration of 1.0 mCi/ml in 0.9% sterile saline.
3. Inject 200 µl of the ^{89}Zr-DFO-J591 solution (200 µCi; 7.4 MBq) into the lateral tail vein of the xenograft-bearing mice.[48]
4. At the desired imaging time point (*e.g.,* 12, 24, 48, 72, 96, or 120 hr post-injection), anesthetize the mouse with a 2% isoflurane: oxygen gas mixture.
5. Place the mouse on the bed of the small animal PET scanner, and maintain anesthesia during the scan using a 1% isoflurane: oxygen gas mixture. Prior to placing the animal on the scanner bed, verify anesthesia using the toe-pinch method and apply ophthalmic ointment to the eyes of the mouse to prevent drying during anesthesia.[49]
6. Acquire the PET data for the mouse via a static scan with a minimum of 40 million coincident events using an energy window of 350-700 keV and a coincidence timing window of 6 nsec.[50]
7. After completing the acquisition of the image, do not leave the mouse unattended and do not place it in a cage with other mice until it has regained consciousness.

Representative Results

The first step in this protocol the conjugation of DFO-NCS to the antibody is typically quite robust and reliable. Generally, the purified, chelator-modified immunoconjugate can be obtained in > 90% yield, and using 3 molar equivalents of DFO-NCS in the initial conjugation reaction will yield a degree-of-labeling of the chelator of approximately 1.0-1.5 DFO/mAb. The ^{89}Zr radiolabeling and purification steps of the procedure are likewise straightforward. At the concentrations outlined in the protocol above, radiolabeling yields of > 80% and thus specific activities of > 2.0 mCi/mg are typical after 60 min at RT. The radio-TLC chromatogram of the crude radiolabeling mixture will likely reveal some DTPA-bound $^{89}Zr^{4+}$ that elutes at the solvent front (**Figure 4A**). However, after quenching the reaction with DTPA and purifying the ^{89}Zr-DFO-mAb construct via size exclusion chromatography, the radiochemical purity of the purified, isolated ^{89}Zr-DFO-mAb conjugate should be > 95% (**Figure 4B**). In the event that the radiochemical purity of the isolated ^{89}Zr-DFO-mAb conjugate is less than 95%, the purification procedure should be repeated prior to performing any *in vitro* or *in vivo* experiments.

Moving on to the *in vivo* experiments, in the protocol described above, athymic nude mice bearing PSMA-expressing, LNCaP prostate cancer xenografts were employed to investigate the *in vivo* behavior of ^{89}Zr-DFO-J591. Both acute biodistribution and PET imaging experiments revealed that ^{89}Zr-DFO-J591 clearly delineates the prostate cancer xenografts with excellent image contrast and high tumor-to-background activity ratios (**Figure 5**). The uptake of the radioimmunoconjugate in the tumor is evident as early as 24 hr (20.9% ± 5.6% ID/g), and the activity concentration in the tumor increases to a maximum of 57.5% ± 5.3% ID/g at 96 hr post-injection. As is typical for radioimmunoconjugates, a relatively high concentration of radiotracer is present in the blood at early time points (9.1% ± 5.3% ID/g at 24 hr), followed by a slow decrease in the amount of radioactivity in the blood over the course of the experiment. The non-target tissue with the highest activity concentration was the bone, which displayed uptake values around 10% ID/g throughout the experiment, presumably as a result of the *in vivo* release of the osteophilic cation ^{89}Zr^{4+}. All other organs including heart, lung, liver, spleen, stomach, large and small intestine, kidney, and muscle displayed relatively low activity concentrations, often well below 5% ID/g. As a control, an additional cohort of mice were injected co-injected 300 µg unlabeled DFO-J591 in order to saturate the antigen and thus illustrate selective blocking. Critically, the blocking experiment lowered uptake of the radioimmunoconjugate in the tumor from 48.9% ± 9.3% ID/g to 23.5% ± 11.1% ID/g at 72 hr post-injection, clearly indicating that ^{89}Zr-DFO-J591 selectively targets its antigen.

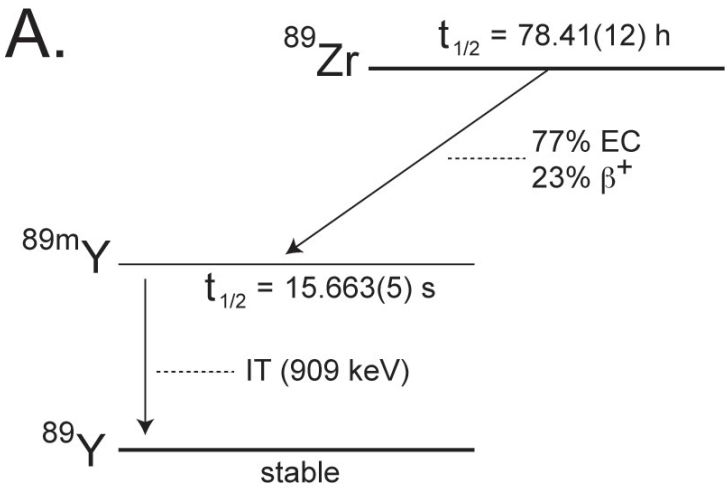

Figure 1. (**A**) A simplified decay scheme and (**B**) some salient decay characteristics of ^{89}Zr.[13,16,17] IT = isomeric transition; EC = electron capture. Modified and reprinted with permission from Deri, *et al. Nuclear Medicine and Biology*. **40**, 3-14 (2013). Please click here to view a larger version of this figure.

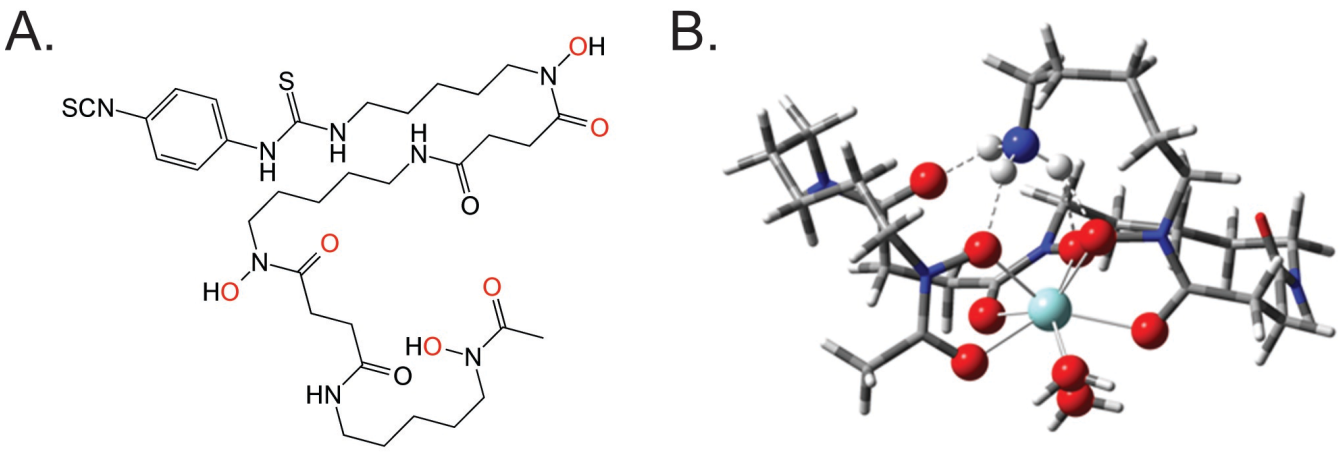

Figure 2. (**A**) The structure of DFO-NCS with the coordinating oxygen atoms colored red; (**B**) A DFT-derived structure of the Zr-DFO coordination complex. Modified and reprinted with permission from Deri, *et al. Journal of Medicinal Chemistry.* **57,** 4849-4860 (2014). Copyright 2014 American Chemical Society. Please click here to view a larger version of this figure.

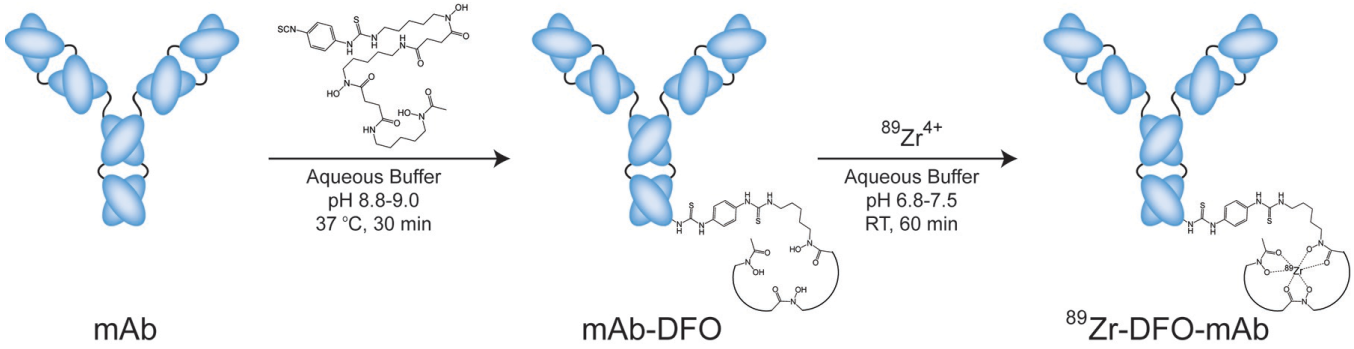

Figure 3. Scheme of the bioconjugation and radiolabeling of ^{89}Zr-DFO-J591. Please click here to view a larger version of this figure.

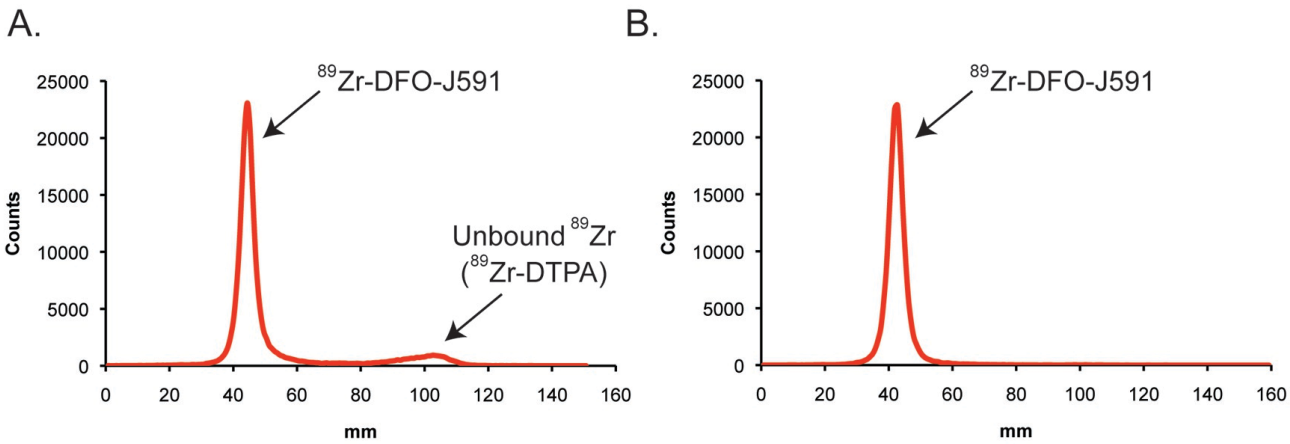

Figure 4. Representative radio-TLC chromatograms of the crude radiolabeling mixture (A) and purified product (B) of ^{89}Zr-DFO-J591. Radio-TLCs were run on silica strips using an eluent of 50 mM DTPA, pH 5.0. Please click here to view a larger version of this figure.

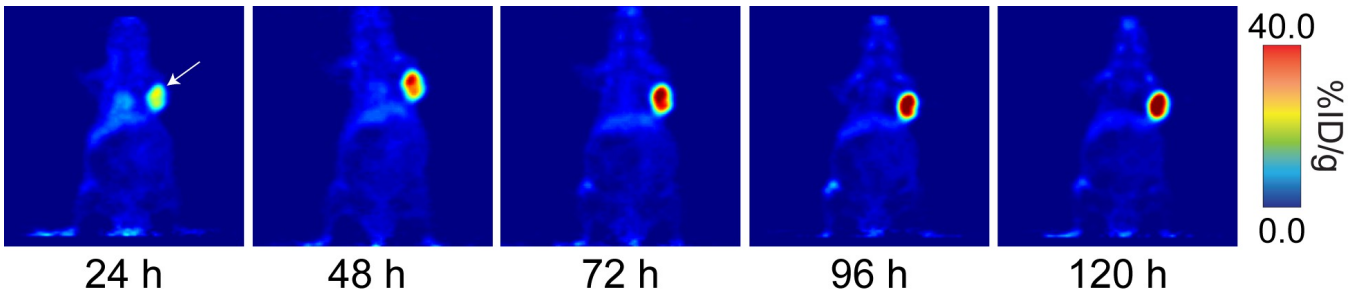

Figure 5. Coronal PET images of ^{89}Zr-DFO-J591 (11.1-12.9 MBq [300-345 µCi] injected via tail vein in 200 µl 0.9% sterile saline) in athymic nude mice bearing subcutaneous, PSMA-expressing LNCaP prostate cancer xenografts (white arrows) between 24 and 120 hr post-injection. Modified and reprinted with permission from Zeglis, *et al. Bioconjugate Chemistry*. **24**, 1057-1067 (2013). Copyright 2013 American Chemical Society. Please click here to view a larger version of this figure.

Discussion

While the construction, radiolabeling, and imaging of ^{89}Zr-DFO-labled radioimmunoconjugates is generally a rather straightforward procedure, it is important to keep a few key considerations in mind during each step of the process. For example, perhaps the most likely cause for concern during the conjugation step of the procedure is the aggregation of the antibody during the conjugation reaction. This problem is most often a product of poor mixing of the conjugation reaction after the addition of the DFO-NCS stock solution.[22] When this happens, the non-homogenous distribution of the DFO-NCS can cause excessively high levels of local reaction with the antibody, which can in turn lead to aggregation. This issue can be relatively easily circumvented by adding the DFO-NCS stock solution in small aliquots (< 5 µl), thoroughly mixing the reaction mixture after the addition of the DFO-NCS, and agitating the reaction mixture on a temperature-controlled shaker. In addition, after the conjugation and purification of the DFO-mAb construct, it is important to precisely determine the number of DFO conjugated to each mAb. The full characterization of the number of DFO chelates per antibody can be achieved using radiometric isotopic dilution experiments similar to those performed by Holland, *et al.* and Anderson, *et al.*, though MALDI-TOF mass spectrometry is a viable alternative.[14,23,30,51,52] During the radiolabeling step, easily the most common problem is lower-than-expected radiolabeling yields. If unexpectedly low yields occur despite assiduously following the protocol above, three different troubleshooting strategies are available: (1) incubating the radiolabeling reaction for

longer amounts of time (*e.g.,* 2-3 hr); (2) repeating the radiolabeling reaction using a higher concentration of antibody; or (3) repeating the initial DFO-NCS conjugation reaction using a higher molar excess of the bifunctional chelator.

While the DFO-NCS conjugation is facile and robust, one of its undeniable weaknesses is that it is not site-specific: DFO-NCS forms thiourea linkages with available lysines in the antibody regardless of their position. As a result, it is possible that the chelators may become appended to the antigen-binding region of the antibody, thereby adversely affecting the immunoreactivity of the ^{89}Zr-DFO-labeled conjugate. Therefore, a fine balance must be struck in the construction of ^{89}Zr-labeled radioimmunoconjugates: higher numbers of chelators per antibody facilitate higher specific activities, but higher degrees of labeling also increase the risk of compromising the immunoreactivity of the construct. In the end, the goal is simple: attach as many chelators as necessary without compromising immunoreactivity. After obtaining the purified ^{89}Zr-DFO-mAb radioimmunoconjugate, it is critical to determine the *in vitro* immunoreactivity of the construct prior to any *in vivo* experimentation. To this end, we recommend using the *in vitro* methods published by Lindmo, *et al.*[53,54] If the immunoreactivity of the construct is lower than 80-90%, it may be necessary to return to the conjugation reaction and append fewer DFO moieties per antibody. Alternatively, if the immunoreactivity of the purified ^{89}Zr-DFO-mAb is high (> 90%) and higher specific activities are desired, it may be possible to attach more chelators to the antibody without decreasing immunoreactivity.

Finally, the *in vivo* behavior of a ^{89}Zr-DFO-labeled antibody is, of course, highly dependent on both the identity of the antibody and the tumor model employed. In the model system presented here, the maximum uptake value in the tumor reaches approximately 60% ID/g; however, reports in the literature for maximum tumor uptake values range from as low as 15-20% ID/g to as high as 80-90% ID/g.[33,44,55-57] Likewise, the amount of uptake in non-target tissues — in particular the liver and spleen — can vary widely depending on the antibody/antigen system being studied. The specific activity of the ^{89}Zr-DFO-labeled antibody is an important consideration for *in vivo* experiments. Literature values for the specific activities of ^{89}Zr-DFO-mAbs typically range from 1-6 mCi/mg (37-222 mBq/mg).[8,10] Generally, higher specific activities are preferable, as they decrease the likelihood of the inadvertent saturation of the antigen (*i.e.,* self-blocking). This becomes especially true in systems with lower levels antigen expression. Regardless of the antibody/antigen system, no *in vivo* investigation of a ^{89}Zr-DFO-labeled imaging agent is complete without a demonstration of selectivity. This can be achieved via blocking experiments using large amounts of unlabeled biomolecule *or* the use of a cell line that does not express the antigen in question. In the procedure described herein, the former was employed, but the selectivity of ^{89}Zr-DFO-J591 has also been demonstrated using PSMA-negative PC3 prostate cancer xenografts.[23]

It is important to note that despite its clear advantages, this DFO-NCS-based synthetic methodology is not perfect. As we have discussed, DFO is not an ideal chelator for $^{89}Zr^{4+}$, and the non-site-specific nature of the conjugation reaction can prove cumbersome. To circumvent these issues, exciting efforts to develop new chelators for $^{89}Zr^{4+}$ and site-specific radiolabeling methodologies are currently underway, yet these new technologies still need to be optimized and validated in both the laboratory and clinic.[24,26,27,29,44] Ultimately, the DFO-NCS methodology for the construction of ^{89}Zr-DFO-labeled antibodies has proven to be an extremely powerful tool for the synthesis of radioimmunoconjugates and has the potential to be used to create a wide variety of clinically useful radiopharmaceuticals.

Disclosures

The authors have nothing to disclose.

Acknowledgements

The authors thank Prof. Thomas Reiner, Dr. Jacob Houghton, and Dr. Serge Lyaschenko for helpful conversations.

References

1. Wu, A. M. Antibodies and antimatter: The resurgence of immuno-PET. *Journal of Nuclear Medicine.* **50**, (1), 2-5 (2009).
2. Wu, A. M., Olafsen, T. Antibodies for molecular imaging of cancer. *Cancer Journal.* **14**, (3), 191-197 (2008).
3. Wu, A. M., Senter, P. D. Arming antibodies: prospects and challenges for immunoconjugates. *Nature Biotechnology.* **23**, (9), 1137-1146 (2005).
4. Zeglis, B. M., Lewis, J. S. A practical guide to the construction of radiometallated bioconjugates for positron emission tomography. *Dalton Transactions.* **40**, (23), 6168-6195 (2011).
5. Zalutsky, M. R., Lewis, J. S. *Handbook of Radiopharmaceuticals.* Welc, M. J., Redvanly, C. S. **24**, 685-714 Wiley New York, NY (2003).
6. Carrasquillo, J. A., *et al.* 124I-huA33 antibody PET of colorectal cancer. *Journal of Nuclear Medicine.* **52**, (8), 1173-1180 (2011).
7. Divgi, C. R., *et al.* Preoperative characterisation of clear-cell renal carcinoma using iodine-124-labelled antibody chimeric G250 (124I-cG250) and PET in patients with renal masses: a phase I trial. *The Lancet Oncology.* **8**, (4), 304-310 (2007).
8. Severin, G. W., Engle, J. W., Barnhart, T. E., Nickles, R. J. Zr-89 radiochemistry for positron emission tomography. *Medicinal Chemistry.* **7**, (5), 389-394 (2012).
9. Nayak, T. K., Brechbiel, M. W. Radioimmunoimaging with longer-lived positron-emitting radionuclides: potentials and challenges. *Bioconjugate Chemistry.* **20**, (5), 825-841 (2009).
10. Vugts, D. J., Van Dongen, G. 89Zr-labeled compounds for PET imaging guided personalized therapy. *Drug Discovery Today.* **8**, (2), e53-e61 (2011).
11. Dongen, G. A. M. S., Visser, G. W. M., de Hooge, M. N. L. ub-, de Vries, E. G., Perk, L. R. Immuno-PET: a navigator in monoclonal antibody development and applications. *Oncologist.* **12**, (12), 1379-1389 (2007).
12. Deri, M. A., Zeglis, B. M., Francesconi, L. C., Lewis, J. S. PET imaging with 89Zr: From radiochemistry to the clinic. *Nuclear Medicine and Biology.* **40**, (1), 3-14 (2013).
13. Holland, J. P., Williamson, M. J., Lewis, J. S. Unconventional nuclides for radiopharmaceuticals. *Molecular Imaging.* **9**, (1), 1-20 (2010).
14. Holland, J. P., Sheh, Y. C., Lewis, J. S. Standardized methods for the production of high specific-activity zirconium-89. *Nuclear Medicine and Biology.* **36**, (7), 729-739 (2009).

15. Meijs, W. E., *et al.* Production of highly pure no-carrier added 89Zr for the labelling of antibodies with a positron emitter. *Applied Radiation and Isotopes.* **45**, (12), 1143-1147 (1994).
16. Vugts, D. J., van Dongen, G. A. M. S. 89Zr-labeled compounds for PET imaging guided personalized therapy. *Drug Discovery Today: Technologies.* **8**, (2-4), e53-e61 (2011).
17. Severin, G. W., Engle, J. W., Barnhart, T. E., Nickles, R. J. 89Zr radiochemistry for positron emission tomography. *Medicinal Chemistry.* **11**, (7), 389-394 (2011).
18. Perk, L. R., *et al.* Quantitative PET imaging of Met-expressing human cancer xenografts with 89Zr-labelled monoclonal antibody DN30. *European Journal of Nuclear Medicine and Molecular Imaging.* **35**, (10), 1857-1867 (2008).
19. Knowles, S. M., *et al.* Quantitative immunoPET of prostate cancer xenografts with Zr-89- and I-124-labeled anti-PSCA A11 minibody. *Journal of Nuclear Medicine.* **55**, (3), 452-459 (2014).
20. Rizvi, S. F., *et al.* radiation dosimetry and scouting of 90Y-ibritumomab tiuxetan therapy in patients with relapsed B-cell non-Hodgkin's lymphoma using 89Zr-ibritumomab tiuxetan and PET. *European Journal of Nuclear Medicine and Molecular Imaging.* **39**, (3), 512-520 (2012).
21. Perk, L. R., *et al.* Preparation and evaluation of Zr-89-Zevalin for monitoring of Y-90-Zevalin biodistribution with positron emission tomography. *European Journal of Nuclear Medicine and Molecular Imaging.* **33**, (11), 1337-1345 (2006).
22. Vosjan, M., *et al.* Conjugation and radiolabeling of monoclonal antibodies with zirconium-89 for PET imaging using the bifunctional chelate p-isothiocyanatobenzyl-desferrioxamine. *Nature Protocols.* **5**, (4), 739-743 (2010).
23. Holland, J. P., *et al.* Zr-89-DFO-J591 for ImmunoPET of prostate-specific membrane antigen expression in vivo. *Journal of Nuclear Medicine.* **51**, (8), 1293-1300 (2010).
24. Deri, M. A., *et al.* Alternative chelator for (89)Zr-radiopharmaceuticals: Radiolabeling and evaluation of 3,4,3-(LI-1,2-HOPO). *Journal of Medicinal Chemistry.* **57**, (11), 4849-4860 (2014).
25. Abou, D. S., Ku, T., Smith-Jones, P. M. In vivo biodistribution and accumulation of 89Zr in mice. *Nuclear Medicine and Biology.* **38**, (5), 675-681 (2011).
26. Guerard, F., Lee, Y. S., Brechbiel, M. W. Rational design, synthesis, and evaluation of tetrahydroxaminc acid chelators for stable complexation of zirconium(IV). *Chemistry: A European Journal.* **20**, (19), 5584-5591 (2014).
27. Guerard, F., *et al.* Investigation of Zr(IV) and 89Zr(IV) complexation with hydroxamates: progress towards designing a better chelator than desferrioxamine B for immuno-PET imaging. *Chemical Communications.* **49**, (10), 1002-1004 (2013).
28. Zeglis, B. M., *et al.* Modular strategy for the construction of radiometalated antibodies for positron emission tomography based on inverse electron demand Diels-Alder click chemistry. *Bioconjugate Chemistry.* **22**, (10), 2048-2059 (2011).
29. Tinianow, J. N., *et al.* Site-specifically Zr-89-labeled monoclonal antibodies for ImmunoPET. *Nuclear Medicine and Biology.* **37**, (3), 289-297 (2010).
30. Holland, J. P., *et al.* Measuring the pharmacodynamic effects of a novel Hsp90 inhibitor on HER2/neu expression in mice using Zr-89-DFO-trastuzumab. *PLoS ONE.* **5**, (1), (2010).
31. Aerts, H., *et al.* Disparity between in vivo EGFR expression and Zr-89-labeled cetuximab uptake assessed with PET. *Journal of Nuclear Medicine.* **50**, (1), 123-131 (2009).
32. Nagengast, W. B., *et al.* Zr-89-Bevacizumab PET of early antiangiogenic tumor response to treatment with HSP90 inhibitor NVP-AUY922. *Journal of Nuclear Medicine.* **51**, (5), 761-767 (2010).
33. Nagengast, W. B., *et al.* In vivo VEGF imaging with radiolabeled bevacizumab in a human ovarian tumor xenograft. *Journal of Nuclear Medicine.* **48**, (8), 1313-1319 (2007).
34. Dijkers, E. C. F., *et al.* Development and characterization of clinical-grade Zr-89-trastuzumab for HER2/neu immunoPET imaging. *Journal of Nuclear Medicine.* **50**, (6), 974-981 (2009).
35. Ulmert, D., *et al.* Imaging androgen receptor signaling with a radiotracer targeting free prostate-specific antigen. *Cancer Discovery.* **2**, (4), 320-327 (2012).
36. Hong, H., *et al.* Positron emission tomography imaging of CD105 expression with 89Zr-Df-TRC105. *European Journal of Nuclear Medicine and Molecular Imaging.* **39**, (1), 138-148 (2012).
37. Dijkers, E. C., *et al.* Biodistribution of Zr-89-trastuzumab and PET omaging of HER2-positive lesions in patients with metastatic breast cancer. *Clinical Pharmacolog., & Therapeutics.* **87**, (5), 586-592 (2012).
38. Heneweer, C., Holland, J. P., Divilov, V., Carlin, S., Lewis, J. S. Magnitude of enhanced permeability and retention effect in tumors with different phenotypes: Zr-89-abumin as a model system. *Journal of Nuclear Medicine.* **52**, (4), 625-633 (2011).
39. Holland, J. P., *et al.* Annotating MYC status with 89Zr-transferrin imaging. *Nature Medicine.* **18**, (10), 1586-1591 (2012).
40. Jacobson, O., *et al.* MicroPET imaging of integrin avB3 expressing tumors using 89Zr-RGD peptides. *Molecular Imaging and Biology.* **13**, (6), 1224-1233 (2011).
41. Keliher, E. J., *et al.* 89Zr-labeled dextran nanoparticles allow in vivo macrophage imaging. *Bioconjugate Chemistry.* **22**, (12), 2383-2389 (2011).
42. Abou, D. S., *et al.* 89Zr-labeled paramagnetic octreotide-liposomes for PET-MR imaging of cancer. *Pharmaceutical Research.* **30**, (3), 878-888 (2013).
43. Miller, L., *et al.* Synthesis, characterization, and biodistribution of multiple 89Zr-labeled pore-expanded mesoporous silica nanoparticles for PET. *Nanoscale.* **6**, (9), 4928-4935 (2014).
44. Zeglis, B. M., *et al.* An enzyme-mediated methodology for the site-specific radiolabeling of antibodies based on catalyst-free click chemistry. *Bioconjugate Chemistry.* **24**, (6), 1057-1067 (2013).
45. Nanus, D. M., *et al.* Clinical use of monoclonal antibody HuJ591 therapy: targeting prostate specific membrane antigen. *Journal of Urology.* **170**, (6 Pt 2), S84-S88 (2003).
46. Joshi, R., Gangabhagirathi, R., Venu, S., Adhikari, S., Mukherjee, T. Antioxidant activity and free radical scavenging reactions of gentisic acid: in vitro and pulse radiolysis studies. *Free Radical Research.* **46**, (1), 11-20 (2012).
47. Saran, M., Bors, W. Radiation chemistry of physiological saline reinvestigated: evidence that chloride-derived intermediates play a key role in cytotoxicity. *Radiation Research.* **147**, (1), 70-77 (1997).
48. Machholz, E., Mulder, G., Ruiz, C., Corning, B. F., Prichett-Corning, K. R. Manual restraint and common compound administration routes in mice and rats. *Journal of Visualized Experiments.* (67), e2771 (2012).
49. Collier, H., Warner, B. T., Skerry, R. Multiple toe-pinch method for testing analgesic drugs. *British Journal of Pharmacology and Chemotherapeutics.* **17**, 28-40 (1961).

50. Zanzonico, P. Positron emission tomography: a review of basic principles, scanner design and performance, and current systems. *Seminars in Nuclear Medicine.* **34**, (2), 87-111 (2004).
51. Anderson, C. J., *et al.* Copper-64-labeled antibodies for PET imaging. *Journal of Nuclear Medicine.* **33**, (9), 1685-1691 (1992).
52. Anderson, C. J., *et al.* Preparation, biodistribution and dosimetry of copper-64-labeled anti-colorectal carcinoma monoclonal antibody fragments 1A3-F(ab')2. *Journal of Nuclear Medicine.* **36**, (5), 850-858 (1995).
53. Lindmo, T., Boven, E., Cuttitta, F., Fedorko, J., Bunn, P. A. Determination of the immunoreactive fraction of radiolabeled monoclonal antibodies by linear extrapolation to binding at infinite antigen excess. *Journal of Immunological Methods.* **72**, (1), 77-89 (1984).
54. Lindmo, T., Bunn, P. A. Determination of the true immunoreactive fraction of monoclonal antibodies after radiolabeling. *Methods in Enzymology.* **121**, (1), 678-691 (1986).
55. Cohen, R., *et al.* Inert coupling of IRDye800CW to monoclonal antibodies for clinical optical imaging of tumor targets. *European Journal of Nuclear Medicine and Molecular Imaging.* **1**, (1), 31-43 (2011).
56. Ruggiero, A., *et al.* Targeting the Internal Epitope of Prostate-Specific Membrane Antigen with Zr-89-7E11 Immuno-PET. *Journal of Nuclear Medicine.* **52**, (10), 1608-1615 (2011).
57. Nayak, T. K., Garmestani, K., Milenic, D. E., Brechbiel, M. W. *PET and MRI of Metastatic Peritoneal and Pulmonary Colorectal Cancer in Mice with Human Epidermal Growth Factor Receptor 1-Targeted Zr-89-Labeled Panitumumab. Journal of Nuclear Medicine.* **53**, (1), 113-120 (2012).

